

## Isolated sub-50 attosecond pulse generation in the combined mid-infrared laser field

Gang-Tai Zhang<sup>a,\*</sup>, Ting-Ting Bai<sup>b</sup>, and Mei-Guang Zhang<sup>a</sup>

<sup>a</sup> Department of Physics and Information Technology, Baoji University of Arts and Sciences, Baoji 721016, China

<sup>b</sup> Department of Mathematics, Baoji University of Arts and Sciences, Baoji 721013, China

Received 1 July 2012; Accepted (in revised version) 30 July 2012

Published Online 28 June 2013

---

**Abstract.** We theoretically study high-order harmonic and isolated attosecond pulse generation from a model helium ion in the combination of the mid-infrared (mid-IR) laser and an extreme ultraviolet (xuv) pulse. It is shown that, for the low laser intensity, the harmonic cutoff is at about 657th order, and the supercontinuum with a 287-eV bandwidth is formed. For the high laser intensity, the spectral cutoff is enlarged to 1795th order, and the supercontinuum is broadened to 834 eV. In the two cases, both the long quantum path selection and the enhancement of the supercontinuum are achieved. Especially for the relatively high laser intensity, pure isolated sub-50 as pulses can be directly obtained by superposing an arbitrary 87-eV harmonics in the supercontinuum from 450th to 1590th order.

**PACS:** 42.65.Ky, 32.80.Rm, 42.65.Re

**Key words:** high-order harmonic generation, supercontinuum, isolated attosecond pulse, combined field

---

## 1 Introduction

Attosecond (as) extreme ultraviolet pulses open the way to a new field of studying and operating basic ultrafast electronic processes in atoms and molecules with an unprecedented precision [1-3]. Thus the generation of attosecond pulse has attracted a great deal of attention in recent years. Since HHG covers a large spectral range from the infrared to soft x-ray region, it has become a candidate for breaking through the femtosecond (fs) limit and a preferred light source for realizing the attosecond pulse generation. Additionally, the HHG is currently the most promising way to produce isolated attosecond

---

\*Corresponding author. *Email addresses:* gtzhang79@163.com (G. -T. Zhang), btt1120@163.com (T. -T. Bai)

pulses in experiments [4,5]. The physical mechanism of the HHG can be well understood by semiclassical three-step model [6]. In detail, the electron first tunnels through the barrier formed by the Coulomb potential and the laser field, then it oscillates almost freely in the laser field, and finally it may recombine with the parent ion and emit a harmonic photon with energy up to  $I_p+3.17U_p$ , where  $I_p$  is the atomic ionization potential and  $U_p=9.38\times 10^{-14}I[\text{W}/\text{cm}^2](\lambda[\mu\text{m}])^2$  is the ponderomotive energy. Since the maximal photon energy scales as the intensity of the driving field or the square of the driving field wavelength, the harmonic cutoff can be extended by enhancing the intensity of the driving field or adopting longer-wavelength driving field. However, on the one hand, too high driving field will result in the ionization saturation of the target atom and limit the harmonic yields; on the other hand, high ionization rate also leads to plasma defocusing of the driving pulse and dephasing of the atomic dipole oscillators, then further decreases the conversion efficiency [7]. Therefore, an efficient method for significantly extending the harmonic cutoff is to adopt a longer-wavelength driving field. With the rapid development of ultrafast laser technology, mid-IR laser pulses with high intensity level can be produced by high-power femtosecond optical parametric amplifiers (OPAs) [8-10]. It has been shown that, by using the mid-IR pulses at wavelengths of 1.51 and 2  $\mu\text{m}$ , the harmonic cutoff energies can be extended to 160 eV [9] and 220 eV [10], respectively. Tate *et al.* [11] has theoretically shown that a mid-IR driving pulse not only produces much more energetic harmonic photons but also reduces harmonic chirps, which is helpful to the attosecond pulse generation.

As is well known, during the recombination in the HHG, a photon is emitted. Usually, this process periodically occurs every half optical cycle, leading to the generation of an attosecond pulse train (APT). For practical application, the straightforward attosecond metrology prefers an isolated attosecond pulse, so much effort has been paid out to obtain an isolated attosecond pulse. It has been shown that an isolated attosecond pulse can be generated by using a few-cycle laser pulse [12,13] or polarization gating technique [14]. In a recent breakthrough work, an isolated attosecond light pulse lasting approximately 80 as were produced with a 3.3 fs, 720 nm laser pulse [15]. However, the duration of isolated attosecond pulse is still significantly longer than the time scale of electron motion in atoms, i.e., 24 as. To broaden the bandwidth of supercontinuum and compress the pulse duration, some other methods have been put forward to reach the desired objectives. It has been proposed that the two-color field can broaden the bandwidth of the supercontinuum spectrum and obtain an isolated attosecond pulse with much shorter duration. Zeng *et al.* [16] theoretically proved that a synthesized two-color field can broaden the bandwidth of the supercontinuum to 148 eV, and then an isolated 65 as pulse was created directly. Lan *et al.* [17] proposed a method for coherently controlling electron dynamics using a few-cycle laser pulse in combination with a controlling field, and also showed that this method not only can broaden the attosecond pulse bandwidth and reduce the harmonic chirp, but also can produce a close-to-Fourier-limit 80-as pulse. An alternative method for generating a broadband attosecond pulse is controlling quantum paths. Macroscopically, the short path can be selected by carefully adjusting the phase-matching

condition [18,19] or spatial filtering [20]. For the single-atom response, the quantum path control can be realized by using the ultrashort pulse [21], two-color field [22-24], three-color field [25,26], an APT [27], or a static electric field [28,29].

In our previous works [30,31], by adding a xuv pulse or a static field to the two-color field, we obtained an isolated 39 or 26 as pulse. Based on these works, in this paper, we investigate the HHG of a model helium ion in the mid-IR laser in combination with a xuv pulse. It is shown that by selecting a proper time delay, not only the conversion efficiency of the harmonics is enhanced, but also the ultrabroad supercontinuum with single quantum path contribution is generated. When the intensity of the mid-IR laser pulse is relatively high, both the harmonic cutoff and the supercontinuum are remarkably extended. By superposing an arbitrary 87-eV harmonics in the supercontinuum from 450th to 1590th order, isolated sub-50 as pulses are obtained directly. These results can be explained in terms of the time–frequency analysis method and the three-step model.

## 2 Theoretical model and methods

In order to verify our scheme, we investigate the HHG spectrum and the attosecond pulse generation by numerically solving the one-dimensional time-dependent Schrödinger equation with the splitting operator method [32]. The harmonic spectrum is obtained by Fourier transforming the time-dependent dipole acceleration of a model atom. The temporal profiles of attosecond pulses can be derived by simply performing inverse Fourier transformation of the XUV supercontinuum in different spectral regions. In our simulation, we choose a soft-core Coulomb potential model  $V(x) = -z/\sqrt{x^2+a}$  and set  $z=2$  and  $a=0.5$  corresponding to the binding energy of 54.4 eV for the ground state of a helium ion ( $\text{He}^+$ ). The driving pulse is consisted of a 12.5 fs/2000 nm mid-IR laser and a 0.9 fs/29.6 nm xuv pulse, and the corresponding electric field is expressed as

$$E(t) = E_0 f_0(t) \cos(\omega_0 t) + E_{\text{xuv}} f_{\text{xuv}}(t - \tau_{\text{delay}}) \cos[\omega_{\text{xuv}}(t - \tau_{\text{delay}})], \quad (1)$$

where  $E_i$  and  $\omega_i$  ( $i=0, \text{xuv}$ ) are the electric field amplitudes and the frequencies of the mid-IR laser and the xuv pulse, respectively.  $f_i(t) = \exp[-4\ln 2(t/\tau_i)^2]$  ( $i=0, \text{xuv}$ ) are the envelopes of the two laser pulses, and  $\tau_i$  ( $i=0, \text{xuv}$ ) are the corresponding pulse durations (full width at half maximum).  $\tau_{\text{delay}}$  is the time delay of the xuv pulse with respect to the mid-IR laser pulse.

## 3 Results and discussion

Fig. 1(a) shows the HHG spectra of  $\text{He}^+$  ion in one-color field and in the combined field of the mid-IR laser pulse and a xuv pulse, respectively. Here the intensities of the mid-IR laser and xuv pulses are  $3 \times 10^{14} \text{ W/cm}^2$  and  $2 \times 10^{13} \text{ W/cm}^2$ , respectively. For the case of single mid-IR laser pulse, the HHG spectrum presents a three-plateau structure, and

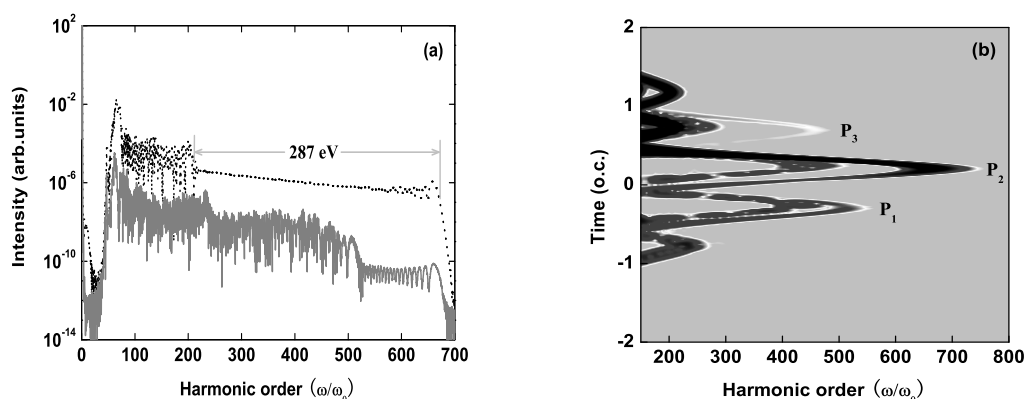


Figure 1: (a) HHG spectra in one-color field (solid curve) and in the combined field of the mid-IR laser and a xuv pulse at a proper time delay of  $\tau_{\text{delay}} = -0.6$  o.c. (dotted curve). (b) Time-frequency distribution of the HHG spectrum corresponding to the dotted curve in (a). The intensities of the mid-IR laser and xuv pulses are  $3.0 \times 10^{14} \text{ W/cm}^2$  and  $2.0 \times 10^{13} \text{ W/cm}^2$ , respectively. o.c. represents the optical cycle of the mid-IR laser pulse.

the spectral cutoff is at approximately the 657th-order harmonic, and the harmonics only in the third plateau is smooth. In addition, the conversion efficiency of supercontinuum is very low, and the supercontinuum shows a strongly modulated structure resulting from the interference of the long and short quantum paths, which is not beneficial for the generation of an isolated attosecond pulse. By adding a 0.9 fs/29.6 nm xuv pulse to the mid-IR pulse at  $\tau_{\text{delay}} = -0.6$  o.c., the situation is completely different, and the result is shown by the dotted curve in Fig. 1(a). As shown in the figure, the overall harmonic spectrum is heightened, only does a two-plateau exist. The spectrum cutoff is still at the 657th-order harmonic and has no distinct change. This is because the contribution of the xuv pulse to the ponderomotive energy is very small, so its contribution can be ignored. It is worth while noting that for the combined field case the harmonic spectrum is more regular and smoother, thus a broad supercontinuum covering a 287 eV bandwidth is formed in the second plateau. Moreover, compared with the case of the mid-IR pulse alone, the bandwidth of the supercontinuum is much broadened and the harmonic intensity is effectively enhanced by 2-5 orders of magnitude. We also note that the modulation of the supercontinuum is weakened, which implies that a single quantum path is selected by use of the xuv pulse.

In order to well understand the spectrum structure, we investigate the emission times of the harmonics for the case in terms of the time-frequency analysis method [33], the result is shown in Fig. 1(b). Clearly, there are three main peaks contributing to the HHG (marked as  $P_1$ ,  $P_2$ , and  $P_3$ ), and the maximal harmonic orders for  $P_1$ ,  $P_2$ , and  $P_3$  are 450, 657, and 500, respectively. The intensity of  $P_2$  is quite strong, whereas the high frequency components of  $P_1$  and  $P_3$  are much weaker than  $P_2$  in the harmonic intensity, so their contribution to the HHG can be ignored. Taking these results into consideration, the

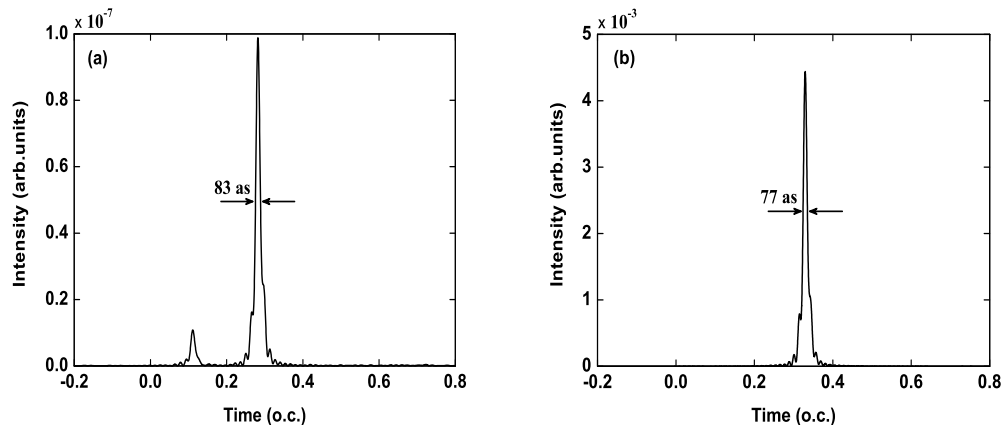


Figure 2: (a) Temporal profile of the attosecond pulse by superposing the harmonics from 530th to 605th order in one-color field. (b) Temporal profile of the attosecond pulse by superposing the harmonics from 400th to 485th order in the combined field. Other parameters are the same as in Fig. 1.

harmonics higher than 210th order are mainly contributed by  $P_2$ , resulting in a supercontinuum with a bandwidth of 287 eV. Note that the bandwidth of the supercontinuum is much broader than that in classical calculation, this is due to the fact that the effect of the ionization probability on the harmonic efficiency is considered in quantum calculation. Furthermore, for the peak  $P_2$ , the intensity of the long quantum path is much higher than that of the short one, i.e., the long quantum path is selected to effectively contribute to the HHG emission.

Through the above analysis, by the use of the xuv pulse, the enhancement of the HHG and the broadband supercontinuum with single quantum path contribution are achieved, which can support the generation of an intense isolated attosecond pulse. In order to check this viewpoint, we investigate the attosecond pulse generation in the combined field. For comparison, we also present the temporal profile of the attosecond pulse in one-color field. As shown in Fig. 2(a), two attosecond bursts are produced by superposing the harmonics from 530th to 605th order, and the duration of the main attosecond pulse is 83 as. Further, before the main pulse, there is a satellite pulse originating from the short quantum path, which indicates that for the one-color field case the harmonics are not locked in phase. For the case of the combined field, by selecting the harmonics from 400th to 485th order, an isolated 77 as pulse with a clean temporal profile is directly obtained, indicating the harmonics in the second plateau are well phase-locked. In addition, the intensity of the generated isolated attosecond pulse is 4 orders of magnitude higher than that in one-color field case, which is attributed to the enhancement of the supercontinuum.

In our simulation, we find that by increasing the intensity of the mid-IR laser pulse, not only the harmonic cutoff and the supercontinuum spectral width can be significantly extended, but also an isolated attosecond pulse with much shorter duration can be ob-

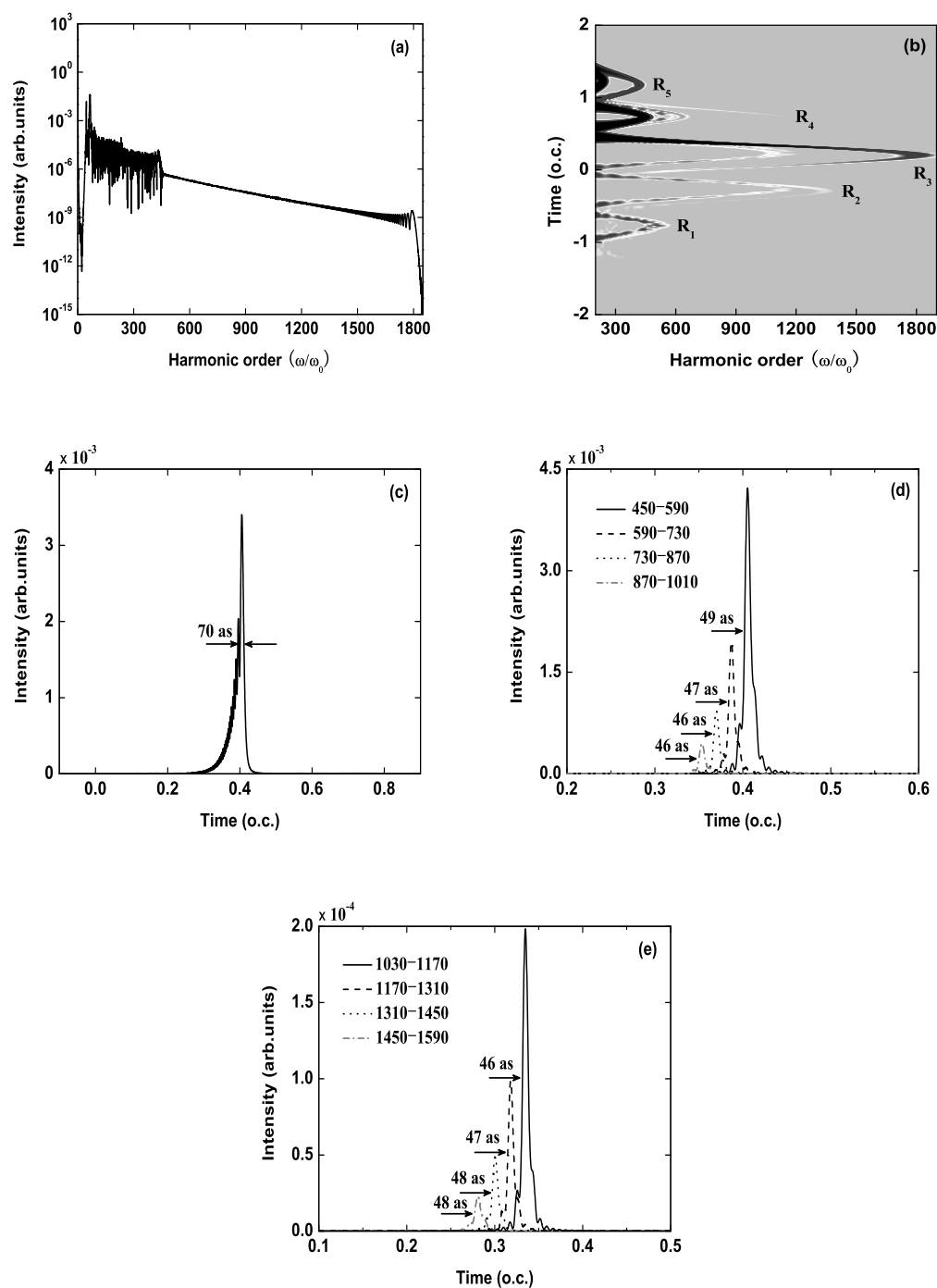


Figure 3: (a) HHG spectrum. (b) Time-frequency distribution of the HHG spectrum corresponding to (a). (c) Temporal profile of the attosecond pulse by superposing the harmonics from 450th to 1795th order. (d) and (e) are the temporal profiles of the attosecond pulses by superposing an arbitrary 87 eV harmonics in the supercontinuum from 450th to 1590th order, respectively. The intensity of the mid-IR laser pulse is  $9.0 \times 10^{14}$  W/cm<sup>2</sup>. Other parameters are the same as in Fig. 1.

tained. Here, the intensity of the mid-IR laser pulse is  $9.0 \times 10^{14}$  W/cm<sup>2</sup>. Other parameters are the same as in Fig. 1. Fig. 3 presents our calculated results for the case. As shown in Fig. 3(a), the harmonic spectrum exhibits a double-plateau structure with two cutoffs: one is at the 433rd order harmonic, the other is at the 1795th order harmonic. The harmonics in the second plateau are regular and smooth, implying that there is only a dominant quantum path contributing to these harmonics. Fig. 3(b) shows the corresponding time-frequency distribution. From this figure, one can see clearly that the harmonics above  $450\omega_0$  mainly originate from the contribution of the peak R<sub>3</sub>, which results in the supercontinuum with a bandwidth of 834 eV. For the peak R<sub>3</sub>, although there are two dominant quantum paths with different emission times contributing to the same harmonic, the long quantum path is much higher than the short one in the intensity, thus the supercontinuum are mainly contributed by the long quantum path. As a result, the harmonics beyond  $450\omega_0$  are almost emitted once, i.e., these harmonics are well phase-locked. Since these phase-locked harmonics cover an extremely broad bandwidth, an ultrashort isolated attosecond pulse can be generated. Fig. 3(c) presents the temporal profile of the attosecond pulse by superposing the harmonics from 450th to 1795th order. As shown in this figure, a single 70 as pulse with several small subpeaks is generated, whereas the intensity ratio of the strongest subpeak to the main pulse is approximately 60%. We also show that pure isolated sub-50 as pulses can be directly produced by superposing an arbitrary 87-eV harmonics in the supercontinuum region from 450th to 1590th order [see Figs. 3(d) and 3(e)], which provides a convenient to obtain an isolated attosecond light pulse with stable pulse duration and tunable central wavelength in experiment. Moreover, it can be seen from Figs. 3(d) and 3(e) that the intensity of the isolated attosecond pulse decreases with increasing the central frequency, this is due to the decrease of the harmonic intensity. The above results also indicate that a short isolated attosecond pulse can be obtained by superposing several high harmonics which agrees with the conclusion of Ref. [4]. As has been reported in Ref. [4], since high harmonics are not synchronized on an attosecond time scale, selecting entire available spectral range no longer provides the shortest possible pulses due to the time-phase dispersion.

To further understand the physical mechanism of the HHG process and the enhancement of the conversion efficiency of the harmonics, we perform the classical trajectory simulation by the three-step model and calculate the ionization probability in the combined field. Laser parameters are the same as in Fig. 3, and the results are shown in Fig. 4. Fig. 4(a) shows the dependence of the kinetic energy on the ionization (gray diamonds) and emission times (black circles). Fig. 4(b) presents the electric field (solid curve) and the dependence of the ionization probability on the time (dotted curve) in the combined field. As shown in Fig. 4(a), there are five ionization peaks contributing to the harmonics, which are marked as R<sub>1</sub>, R<sub>2</sub>, R<sub>3</sub>, R<sub>4</sub>, and R<sub>5</sub>, respectively. The maximum kinetic energies of R<sub>1</sub>, R<sub>2</sub>, R<sub>3</sub>, R<sub>4</sub>, and R<sub>5</sub> are 260 eV, 769 eV, 1059 eV, 675 eV, and 199 eV, respectively. Since the maximum kinetic energy of the electron gained from the laser field is expanded to 1059 eV, the spectral cutoff for the case is greatly extended to  $I_p + 1059$  eV (i.e.,  $1795\omega_0$ ). Note that, in our simulation, the intensity of the laser pulse is

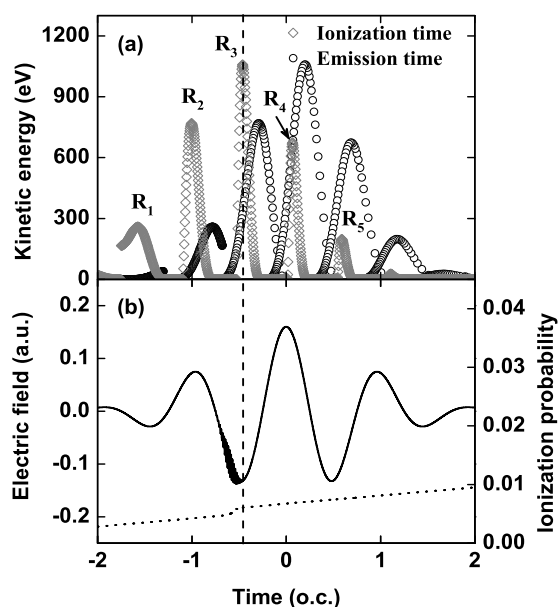


Figure 4: (a) Dependence of the kinetic energy on the ionization (gray diamonds) and emission times (black circles) in the combined field. (b) Electric field (solid curve) and dependence of the ionization probability on the time (dotted curve) in the combined field. Laser parameters are the same as in Fig. 3.

far below the saturation intensity of the  $\text{He}^+$  ion, thus the harmonic efficiency is mainly determined by the ionization rate according to the three-step model. Though there are four ionization peaks occurring at -1.58 o.c., -1.0 o.c., -0.07 o.c., and 0.6 o.c., respectively, the corresponding ionization takes place very slowly, as shown by the dotted curve in Fig. 4(b). Thus the contribution of the four peaks to the HHG can be ignored. For the peak R<sub>3</sub>, there are two classical electron paths corresponding to the same kinetic energy. A path with earlier ionization time but later emission time is called the long path, and a path with later ionization time but earlier emission time is called the short path. In our scheme, the supercontinuum is mainly attributed to the ionized electrons in the time range from -0.52 to -0.26 o.c.. Electrons with the long paths are mainly ionized from -0.52 to -0.46 o.c., and electrons with the short paths are mainly ionized from -0.46 to -0.26 o.c., however, the ionization probability of electrons in the time range from -0.6 to -0.46 o.c. increases rapidly. Thus the long path dominates over the short path for the supercontinuum generation. In addition, the ionization takes place rapidly at -0.6 o.c., which means that the ionization rate of the electrons contributing to the supercontinuum is greatly increased, resulting in the efficient enhancement of the supercontinuum. Indeed, the 29.6 nm xuv pulse holds a 41.86 eV photon energy, which is close to the  $1s-2p$  the transition energy (40.8 eV) for  $\text{He}^+$  as reported in Ref. [34]. But for our model  $\text{He}^+$  ion, the 29.6 nm xuv pulse can promote a resonance transition from the ground state to the second excited

state. The electron populated in the state is easily ionized by the driving field because of the low binding energy. Thus the ionization yields are significantly increased. As a result, the conversion efficiency of the HHG is remarkably enhanced.

## 4 Conclusions

In conclusion, we theoretically present an efficient method to generate an intense isolated attosecond pulse in the combination of the mid-IR laser and a xuv pulse. It is shown that this method can not only enhance the conversion efficiency of the HHG, but also generate a broad supercontinuum. Due to the use of the xuv pulse, the quantum paths of HHG in the single mid-IR laser pulse can be significantly modulated, as a result, a single long quantum path is selected. We also show that, by increasing the intensity of the mid-IR laser pulse, both the extension of the harmonic cutoff and the broadening of the supercontinuum can be achieved. In addition, since the supercontinuum covers an extremely broad bandwidth, isolated sub-50 as pulses can be directly produced by superposing an arbitrary 87-eV harmonics in the supercontinuum region from 450th to 1590th order, which is better for generating isolated attosecond light pulses with stable pulse durations and tunable central wavelengths in experiment. In our scheme, the enhancement of the supercontinuum is much more efficient. This is because the production time and property of the electron wave packet (EWP) can be controlled by the xuv pulse. As a result, the ionization yields of the electrons with a single quantum path can be increased, leading to the supercontinuum with high conversion efficiency. Experimentally, a 12.5 fs, 2000 nm can be generated from the Ti: sapphire laser system via an optical parametric amplifier (OPA), and a 0.9 fs, 29.6 nm xuv pulse can be produced by synthesizing the high-order harmonics such as Refs. [12-15], besides, the time delay between the two pulses can be adjusted by a piezoelectric transducer delay stage [35]. Consequently, the scheme presented here appears feasible for an experimental demonstration in the near future. In short, the advantages of our scheme lie in generating an ultrabroad xuv supercontinuum with single quantum path contribution and maintaining a high conversion efficiency, which are favorable for the production of isolated attosecond pulses.

**Acknowledgments.** This work was supported by the Science Foundation of Baoji University of Arts and Sciences, China (Grant Nos. ZK10122, ZK11061, ZK11135, and ZK11060).

## References

- [1] M. Drescher, M. Hentschel, R. Kienberger, *et al.*, Nature 419 (2002) 803.
- [2] R. Kienberger, E. Goulielmakis, M. Uiberacker, *et al.*, Nature 427 (2004) 817.
- [3] M. Uiberacker, T. Uphues, M. Schultze, *et al.*, Nature 446 (2007) 627.
- [4] Y. Mairesse, A. D. Bohan, L. J. Frasinski, *et al.*, Science 302 (2003) 1540.
- [5] P. M. Paul, E. S. Toma, P. Breger, *et al.*, Science 292 (2001) 1689.

- [6] P. B. Corkum, *Phys. Rev. Lett.* 71 (1993) 1994.
- [7] W. Y. Hong, P. X. Lu, Q. G. Li, and Q. B. Zhang, *Opt. Lett.* 34 (2009) 2102.
- [8] H. Xu, H. Xiong, Z. N. Zeng, *et al.*, *Phys. Rev. A* 78 (2008) 033841.
- [9] B. Shan and Z. H. Chang, *Phys. Rev. A* 65 (2001) 011804.
- [10] P. Colosimo, G. Doumy, C. I. Blaga, *et al.*, *Nat. Phys.* 4 (2008) 386.
- [11] J. Tate, T. Augustine, H. G. Muller, *et al.*, *Phys. Rev. Lett.* 98 (2007) 013901.
- [12] M. Hentschel, R. Kienberger, C. Spielmann, *et al.*, *Nature* 414 (2001) 509.
- [13] A. Baltuška, T. Udem, M. Uiberacker, *et al.*, *Nature* 421 (2003) 611.
- [14] G. Sansone, E. Benedetti, F. Calegari, *et al.*, *Science* 314 (2006) 443.
- [15] E. Goulielmakis, M. Schultze, M. Hofstetter, *et al.*, *Science* 320 (2008) 1614.
- [16] Z. N. Zeng, Y. Cheng, X. H. Song, *et al.*, *Phys. Rev. Lett.* 98 (2007) 203901.
- [17] P. F. Lan, P. X. Lu, W. Cao, *et al.*, *Phys. Rev. A* 76 (2007) 011402(R).
- [18] W. Y. Hong, Q. B. Zhang, Z. Y. Yang, *et al.*, *Phys. Rev. A* 80 (2009) 053407.
- [19] P. Salieres, A. L'Huillier, and M. Lewenstein, *Phys. Rev. Lett.* 74 (1995) 3776.
- [20] R. López-Martens, K. Varj, P. Johnsson, *et al.*, *Phys. Rev. Lett.* 94 (2005) 033001.
- [21] Y. Liu, G. L. Chen, and H. L. Shao, *J. At. Mol. Phys.* 28 (2011) 697 (in Chinese).
- [22] L. Zhang, Y. F. Yang, M. L. Yuan, *et al.*, *J. At. Mol. Phys.* 27 (2010) 275 (in Chinese).
- [23] W. Cao, P. X. Lu, P. X. Lan, *et al.*, *J. Phys. B: At. Mol. Opt. Phys.* 40 (2007) 869.
- [24] Y. H. Guo, R. F. Lu, K. L. Han, and G. Z. He, *Int. J. Quant. Chem.* 109 (2009) 3410.
- [25] A. F. Cao and X. Y. Miao, *J. At. Mol. Phys.* 29 (2012) 86 (in Chinese).
- [26] R. F. Lu, H. X. He, Y. H. Guo, and K. L. Han, *J. Phys. B: At. Mol. Opt. Phys.* 42 (2009) 225601.
- [27] K. J. Schafer, M. B. Gaarde, A. Heinrich, *et al.*, *Phys. Rev. Lett.* 92 (2004) 023003.
- [28] W. Y. Hong, P. X. Lu, P. X. Lan, *et al.*, *Phys. Rev. A* 77 (2008) 033410.
- [29] C. L. Xia, X. L. Ge, Y. S. Wang, and X. S. Liu, *J. At. Mol. Phys.* 29 (2012) 312 (in Chinese).
- [30] G. T. Zhang, J. Wu, C. L. Xia, and X. S. Liu, *Phys. Rev. A* 80 (2009) 055404.
- [31] G. T. Zhang, T. T. Bai, and M. G. Zhang, *Chin. Phys. B* 21 (2012) 054214.
- [32] M. D. Feit, J. A. Fleck, and A. Steiger, *J. Comput. Phys.* 47 (1982) 412.
- [33] P. Antoine and B. Piraux, *Phys. Rev. A* 51 (1995) R1750.
- [34] K. Ishikawa, *Phys. Rev. Lett.* 91 (2003) 043002.
- [35] H. Mashiko, S. Gilbertson, C. Li, *et al.*, *Phys. Rev. Lett.* 100 (2008) 103906.